

Origin of bedding-parallel calcite “beef” layers in the Upper Jurassic Haynesville shale, northwestern Louisiana

L. Taras Bryndzia, Calum I. Macaulay, Alexander P. Litvinchuk, and Brian D. Monteleone

AAPG Bulletin, v. 108, no. 2 (February 2024), pp. 379–400

Copyright ©2024. The American Association of Petroleum Geologists. All rights reserved.

Appendix 1. Stable Carbon, Oxygen, and Sulfur Isotopes

A.1.1. Carbon and Oxygen Isotopes

Compounds $\delta^{13}\text{C}$ and $\delta^{18}\text{O}$ were measured on nine calcite “beef” layers from well 5, including six samples of vertical calcite veins. The isotopic data were collected as part of a Haynesville-Bossier Joint Industry Project managed by CoreLabs (Houston, Texas) and included the 15 samples discussed here that were contributed by Shell to the consortium. Carbon and oxygen isotopic compositions on calcite from bedding-parallel calcite layers (BPCLs) were analyzed by Isotech Laboratories, Champaign, Illinois, using their standard acid digestion and dual inlet-isotope ratio mass spectrometry technique. The data are summarized in Table A1.1.

A.1.2. Sulfur Isotopes

Since the focus of this work involves the analysis and interpretation of sulfur isotopic data of sulfur-bearing species, a short introduction to the nomenclature of sulfur isotope analysis and data interpretation is warranted.

Sulfur ($Z = 16$) has four stable isotopes: ^{32}S , ^{33}S , ^{34}S , and ^{36}S , with approximate terrestrial abundances of 95.02%, 0.75%, 4.21%, and 0.02%, respectively (Macnamara and Thode, 1950).

The primary variable in the analysis and interpretation of sulfur isotopic variations in natural systems involves change in the ratio of $^{34}\text{S}/^{32}\text{S}$ in a sample relative to a reference standard. For most studies, the universal standard for sulfur isotopic data is referred to as the Vienna Canon Diablo Troilite standard (VCDT). The sulfur isotopic composition of a compound is usually expressed as a $\delta^{34}\text{S}$ value, which is defined as a per mil (‰) deviation of the $^{34}\text{S}/^{32}\text{S}$ ratio of the compound relative to that of the troilite phase of the Canon Diablo meteorite ($^{34}\text{S}/^{32}\text{S} = 0.0450045$; Ault and Jensen, 1963; Ohmoto and Rye, 1979).

$$\delta^{34}\text{S}_{\text{sample}} = \left[\left(\frac{^{34}\text{S}/^{32}\text{S}}{\text{sample}} \right) / \left(\frac{^{34}\text{S}/^{32}\text{S}}{\text{standard}} \right) - 1 \right] \times 1000 \quad (\text{A1})$$

This means that the difference (i.e., δ) for VCDT itself has a value of $\delta^{34}\text{S}$ equal to zero.

The primary vendor for the analysis of sulfur isotopic data that forms the basis of this report was performed by Isotech, a commercial vendor laboratory in Champaign, Illinois. One of the initial stages of this project was an attempt to quality control Isotech’s analytical capabilities by comparing their analytical results against a suite of samples that had previously been analyzed at the Lyons Biogeochemistry Laboratory (University of California, Riverside) and found to be both reproducible and reliable standards for this work. The range of sulfur isotopic compositions ranged from approximately -20‰ to $+20\text{‰}$ and included both reduced sulfur phases such as acanthite (Ag_2S) and the oxidized sulfur-bearing phases barite (BaSO_4) and anhydrite (CaSO_4).

Samples of H_2S from Haynesville wells were collected by the senior author during November 2010. The H_2S sulfur was captured as Ag_2S , precipitated by passing a stream of production gas at the separator through a 500-ml Erlenmeyer flask containing 2 M AgNO_3 . The Ag_2S was analyzed at the Lyons Biogeochemistry Laboratory. The results

Table A1.1. Carbon and Oxygen Isotopic Composition of Calcite from Bedding-Parallel Calcite Layers and Vertical Calcite Veins from Well 5 in the Haynesville Shale

| | $\delta^{13}\text{C}$ Calcite, ‰; VPDB | $\delta^{18}\text{O}$ Calcite, ‰; VPDB |
|------------|--|--|
| Horizontal | 4.37 | −9.30 |
| | 4.67 | −8.95 |
| | 2.9 | −10.37 |
| | 3.94 | −10.28 |
| | 4.02 | −10.15 |
| | 3.54 | −10.39 |
| | 2.01 | −10.72 |
| | 4.89 | −9.65 |
| | 4.35 | −9.89 |
| | Vertical | 4.03 |
| 5.78 | | −10.00 |
| 6.49 | | −10.07 |
| 5.78 | | −10.15 |
| 5.71 | | −9.80 |
| 5.19 | | −9.78 |

Abbreviation: VPDB = Vienna Pee Dee belemnite.

Table A1.2. Bulk Sulfur Isotopic Composition of Pyrite, Solid Hydrocarbons, and Anhydrite from the Bossier and Haynesville Shales

| Formation | Well | $\delta^{34}\text{S}$, ‰, VCDT | | | Depth, ft |
|-----------|---------|---------------------------------|-------|-----------|-----------|
| | | Pyrite | SHC | Anhydrite | |
| Bossier | 1 | -13.6 | -11.0 | | 12,374.0 |
| | 1 | -15.5 | -23.9 | | 12,386.7 |
| | 1 | -12.4 | -25.0 | | 12,392.5 |
| | 1 | -11.0 | -18.6 | | 12,421.8 |
| | 1 | -13.3 | -22.5 | | 12,432.9 |
| HSQL | 1 | -13.3 | -15.1 | | 12,465.8 |
| | 1 | -11.1 | -20.2 | | 12,492.9 |
| | 1 | -9.6 | -19.2 | | 12,507.0 |
| | 1 | -12.1 | -16.3 | | 12,522.7 |
| | 1 | -14.5 | | | 12,663.7 |
| | 2 | -9.5 | -18.5 | | 13,218.0 |
| | 2 | -10.6 | | | 13,237.1 |
| | 2 | -9.3 | -20.6 | | 13,248.8 |
| | 2 | -12.5 | -11.3 | | 13,259.9 |
| | 2 | -9.2 | -16.5 | | 13,269.8 |
| | 2 | -8.9 | | | 13,221.3 |
| | 2 | -10.4 | | | 13,235.0 |
| | 2 | -13.0 | | | 13,244.2 |
| | 2 | -12.0 | | | 13,292.3 |
| Bossier | 3 | | -8.3 | | 12,133.3 |
| HSQL | 3 | | 1.9 | | 13,250.1 |
| | 3 | -12.6 | -17.3 | | 12,443.5 |
| | 3 | -15.0 | -33.0 | | 12,459.5 |
| | 3 | -15.3 | | | 12,434.5 |
| | 3 | -19.6 | | | 12,452.0 |
| | 3 | -14.9 | | | 12,481.5 |
| | 3 | -19.6 | | | 12,496.5 |
| | 3 | -19.0 | | | 12,500.0 |
| | 3 | -20.1 | | | 12,502.5 |
| Werner | Crocker | | | 20.2 m | 14,949.1 |
| | Crocker | | | 19.3 m | 14,951.7 |
| | Crocker | | | 18.1 m | 14,951.7 |
| | Crocker | | | 15.8 s | 14,972.1 |
| | Crocker | | | 15.3 s | 14,972.1 |
| | Crocker | | | 16.8 s | 14,996.4 |
| | Crocker | | | 15.9 s | 14,996.4 |

Werner anhydrite textures: (texture: m = massive; s = sucrose).

Abbreviations: SHC = solid hydrocarbons; VCDT = Vienna Canon Diablo Troilite standard.

are reported as deviations in the ratio of $^{32}\text{S}/^{34}\text{S}$ in a sample, relative to the VCDT standard. Reported deviations in the $^{32}\text{S}/^{34}\text{S}$ ratio from both laboratories are $\pm 0.2\text{‰}$.

Sulfur in CaSO_4 sampled from core in the Shell Crocker well was analyzed at Coastal Laboratories in Austin, Texas, as well as at Lyons Biogeochemistry Laboratory and at Iso-labs. All three laboratories used the same methods of extraction and analysis and reported similar analytical uncertainties

in the $^{32}\text{S}/^{34}\text{S}$ ratio of $\pm 0.2\text{‰}$. Interlaboratory comparisons for multiple analyses of the same samples were consistently within $\pm 2\text{‰}$ of one another.

Seven samples of Haynesville core were crushed and soluble sulfate extracted using deionized water at TerraTek Laboratories, Salt Lake City, Utah. The sulfate was precipitated as BaSO_4 by mixing with a BaCl_2 solution. The precipitated barite was analyzed at the Lyons Biogeochemistry Laboratory. The results are summarized in Table A1.3.

A.1.3. Secondary Ion Mass Spectrometry

Ion microprobe analyses of sulfur isotopes in various mineral phases were analyzed at the Northeast National Ion Microprobe Facility located at Woods Hole Oceanographic Institution (WHOI) in Woods Hole, Massachusetts. To determine if the sulfate-bearing veins were contributing to the isotopically light H_2S , we undertook a detailed ion microprobe study of sulfur isotopes in sulfate and pyrite from the BPCLs sampled in 10 wells that penetrated the Haynesville and Bossier shales. The analytical work was performed by Calum I. Macaulay and Brian D. Monteleone (WHOI).

In situ sulfur isotope measurements were made by secondary ion mass spectrometry using a Cameca 1280 ion

Table A1.3. Sulfur Isotopic Composition of H_2S Gas and Sulfate Leached from Samples in Different Wells from the Bossier and Haynesville Shales

| Formation | Well | $\delta^{34}\text{S}$, ‰, VCDT | | Depth, ft |
|-------------|--------|---------------------------------|---------------|-----------|
| | | H_2S | Sulfate Leach | |
| Bossier | D-13 | -13.7 | | 11,548 |
| | D-13 | -14.5 | | 11,548 |
| | JRB | -16.9 | | 12,843 |
| Haynesville | GF-24 | 12.4 | | 12,161 |
| | 8 | | -0.2 | 12,343.5 |
| | | | 0.1 | 12,343.5 |
| | 9 | 14.0 | | 12,248 |
| | 9 | | -4.7 | 12,297.9 |
| | 9 | | 0.7 | 12,322.5 |
| | 9 | | 1.2 | 12,322.5 |
| | 9 | | -11.4 | 12,365.4 |
| | SP-7-2 | 1.2 | | 12,644 |
| | 10 | 16.3 | | 12,206 |
| | 10 | 15.6 | | 12,206 |
| | D-21 | -19.6 | | 12,419 |
| | SF-23 | -20.7 | | 12,214 |
| | SP-7-2 | 1.3 | | 12,644 |
| 2 | 18.7 | | 12,800 | |
| 2 | 18.7 | | 13,200 | |
| 2 | | -5.0 | 13,251 | |
| 2 | | 3.2 | 13,277 | |
| 2 | | 1.7 | 13,301.3 | |

Abbreviation: VCDT = Vienna Canon Diablo Troilite standard.

Table A1.4. Bulk Sulfur Isotopic Analyses of the Shell Potosi Barite Standard as Reported by Lyons Biogeochemistry Laboratory, University of California, Riverside

| Identifier 1 | Sample Mass, mg | Wt. % Sulfur, by EA | Sulfur, μg | $\delta^{34}\text{S}/^{32}\text{S}$, Versus VCDT | Time Code |
|--|-----------------|---------------------|-----------------------|---|---------------------|
| Shell Potosi barite 1 | 0.400 | 13.6 | 54.6 | 24.6 | 10/14/201320:36:31 |
| Shell Potosi barite 2 | 0.4 | 12.9 | 51.5 | 25.4 | 10/14/2013 20:50:27 |
| Shell Potosi barite 3 | 0.389 | 15 | 58.2 | 25.7 | 10/14/2013 21:04:23 |
| Shell Potosi barite 4 | 0.382 | 14.4 | 55.1 | 25.1 | 10/14/2013 21:18:20 |
| Shell Potosi barite 5 | 0.376 | 13.8 | 51.9 | 25.1 | 10/14/2013 21:32:16 |
| Shell Potosi barite 6 | 0.426 | 13.4 | 56.9 | 25.2 | 10/14/2013 21:46:12 |
| Shell Potosi barite 7 | 0.382 | 13.5 | 51.7 | 25.1 | 10/14/2013 22:00:09 |
| Average ($\pm 1\sigma$; $n = 7$) | | | | 25.2 0.3 | |

Abbreviation: VCDT = Vienna Canon Diablo Troilite standard.

microprobe. In this technique, a beam of Cs ions is used to liberate secondary sulfur ions from the sample surface, and the ^{32}S and ^{34}S isotopes are separated by acceleration through a long, curved flight tube with strong magnetic fields before being collected and counted. The samples used were highly polished 1-in. round thin sections, and the analytical spot size on the sample surface was 20 μm . A Cs^+ primary beam was used at currents ranging from 500 pA (for pyrite) to 1 nA (for anhydrite) with electron gun charge neutralization. Typically, a raster of 25 to 30 \times 25 to 30 μm was applied to the primary beam. Analysis included a 240-s presputter, followed by 40 cycles measuring ^{32}S and ^{34}S for 5 and 15 s, respectively. A mechanical field aperture was applied to the magnified secondary ion beam to limit the measured area from the pit to the innermost 8–10 μm . Both ^{32}S and ^{34}S were measured on the 10^{11} -ohm Faraday detectors. The entrance and exit slits were set for a mass resolving power of 4000. Typical alpha values for instrumental mass fractionation derived from standards ($[\text{measured } ^{34}\text{S}/^{32}\text{S}]/[\text{actual } ^{34}\text{S}/^{32}\text{S}]$) were 0.993 for pyrite and 0.970 for barite and anhydrite.

For pyrite standards, we used pyrite from Balmat (Balmat, New York; $\delta^{34}\text{S} +15.1$) and Ruttan (Manitoba, Canada; $\delta^{34}\text{S} +1.2$), which are recognized homogenous standards (Crowe and Vaughn, 1996). The anhydrite standard used was Jurassic Werner anhydrite, with a $\delta^{34}\text{S}$ of +16.6‰ from the Shell Crocker 1 well core that is stored at the Bureau of Economic Geology, The University of Texas at Austin, Austin, Texas. The barite standard was from the Potosi mine, Potosi, Missouri, with a $\delta^{34}\text{S}$ of +25.2‰ (Table A1.4). The reproducibility of the anhydrite and barite standards was tested and confirmed through multiple conventional sulfur isotope analyses made in the Lyons Biogeochemistry Laboratory.

Data reduction included correction for Faraday background, time interpolation to adjust for measurement of ^{32}S and ^{34}S at different times within each cycle, and 2σ filtering for outliers within the 40-cycle measurement. For this, WHOI used an in-house MATLAB code called Dirvit. Most of the crystals were analyzed between one and four

times, depending on the quality of the measurements (i.e., the internal standard deviation).

Before being loaded into the ion microprobe, the samples were coated with a relatively thick (30 nm) layer of Au to ensure a perfectly conductive surface. A consequence of this thick coating of Au is that much of the fine detail on the sample surface is obscured. To mitigate target identification difficulties, each sample was initially sputter coated with a thin layer of Au at Shell Technology Center Houston and mapped in high resolution using scanning electron microscopy (SEM) to ensure that target minerals would be located efficiently with the help of SEM maps once samples were loaded into the ion microprobe. Ion microprobe data are summarized in Table A1.5 and have been included in Figures 4 through 6 in the paper.

Appendix 2. Fluid Inclusion Thermometry

Fluid inclusion (FI) petrography and microthermometry were conducted by Fluid Inclusion Technologies (now SLB, Salt Lake City, Utah), with the goal of determining the temperatures and salinities of aqueous inclusions and temperatures and API gravities of petroleum inclusions wherever possible. The samples were examined in both plain light and under ultraviolet illumination. The FI assemblages were identified according to their presence, relationship to the host, consistency of visual parameters (e.g., apparent liquid/vapor ratio), and applicability for determining the requested information. Inclusions were selected for detailed study based on this initial screening. Aqueous and petroleum inclusion homogenization temperatures and aqueous inclusion salinities were determined with a Fluid Inclusion Technologies–modified US Geological Survey heating-freezing stage using standard techniques. Petroleum inclusion API gravities were determined, where possible, using a proprietary Fluid Inclusion Technologies, Inc. technique.

Table A2.1 contains summaries of FI data from calcite and sulfate minerals in calcite beef layers from wells 1, 2, and 5 in the Haynesville shale. No FI homogenization

Table A1.5. Ion Microprobe Sulfur Isotopic Compositions from Bedding-Parallel Calcite Layers

| Well | Depth, ft | $\delta^{34}\text{S}$, ‰, VCDT | | |
|------------|-----------|---------------------------------|--------|-----------|
| | | Pyrite | Barite | Anhydrite |
| 1 | 12,614.5 | -16.8 | 21.1 | |
| | 12,614.5 | -14.5 | 18.6 | |
| | 12,614.5 | -20.5 | | |
| | 12,614.5 | -12.3 | | |
| | 12,614.5 | -10.5 | | |
| | 12,614.5 | -21.4 | | |
| | 12,614.5 | -17.6 | | |
| | 12,614.5 | -16.8 | | |
| | 12,614.5 | -14.5 | | |
| | 12,614.5 | -20.0 | | |
| 3 | 12,133.3 | -16.0 | 11.9 | |
| | 12,133.3 | | 15.5 | |
| 4 | 12,345.1 | -11.4 | 23.7 | |
| | 12,345.1 | -14.8 | 25.0 | |
| | 12,345.1 | -13.1 | 17.6 | |
| | 12,402.7 | -14.9 | 19.5 | |
| | 12,402.7 | -17.1 | | |
| | 12,402.7 | -14.6 | | |
| 5 | 12,318.7 | -9.9 | 19.5 | 23.6 |
| | 12,316.5 | -9.4 | 19.9 | |
| | 12,316.5 | -11.7 | 19.0 | |
| | 12,316.5 | -10.5 | 25.6 | |
| | 12,355.0 | -10.4 | 19.2 | |
| | 12,355.0 | -9.1 | 23.2 | |
| | 12,355.0 | -11.1 | 19.3 | |
| | 12,355.0 | | 22.4 | |
| 6 | 13,251.7 | -9.1 | 17.3 | |
| | 13,251.7 | -8.7 | 15.7 | |
| | 13,251.7 | -9.1 | 15.5 | |
| 7 | 12,425.5 | -11.7 | 14.0 | |
| | 12,425.5 | -8.2 | 11.9 | |
| | 12,425.5 | -8.1 | 21.7 | |
| | 12,425.5 | -14.2 | 16.4 | |
| 8 | 12,341.8 | -9.3 | 20.2 | |
| | 12,341.8 | -11.0 | 20.2 | |
| 9 | 12,366.9 | -21.1 | 21.9 | |
| | 12,366.9 | -17.8 | 22.4 | |
| NFR Energy | 11,191.0 | -28.5 | | 14.7 |
| Huffman 1 | 11,191.0 | -17.3 | | 14.5 |
| | 11,191.0 | -22.2 | | |
| | 11,191.0 | -12.2 | | |

temperature data are available for well 7 due to the lack of aqueous inclusions. The inclusion population in calcite samples from well 7 were dominated by CH₄ gas inclusions only. An inferred temperature of 160°C was used to interpret the microlaser Raman spectroscopic data in Table A3.2

for estimating in situ CH₄ density for well 7. Table A2.2 presents FI data for a sphalerite-bearing vein in calcite from well 2 that was measured internally at the Shell Technology Center Houston by Calum I. Macaulay.

Appendix 3. Microlaser Raman Spectroscopy

Raman scattering measurements were performed at the University of Houston, Houston, Texas, with a triple Horiba Jobin-Yvon T64000 spectrometer, equipped with a microscope, liquid nitrogen-cooled charge-coupled-device detector, and an Ar⁺ laser ($\lambda_{exc} = 488.0 \text{ nm}$) as the excitation source. The spectral resolution did not exceed 1.2 cm^{-1} . To minimize errors in determining peak shifts, the spectrometer position was always fixed, and spectral lines of Ar⁺ plasma were recorded simultaneously with the spectra of studied samples (Norlen, 1973). Furthermore, peak shifts were determined from the fitting of observed lines to Lorentzian profiles using GRAMS/AI software. As a result, the error in determining peak shifts did not exceed 0.1 cm^{-1} .

The samples analyzed were FI wafers of calcite “beef” as shown in Figures 5, 6, and 12 in the paper. In the case of CH₄, it is accepted practice to use the strongest line in the Raman spectrum, which is due to the symmetric CH₄ bond stretching vibration, as a reference (Lu et al., 2007). We have adopted this methodology, along with our own laboratory calibration for the zero-pressure intercept for the C–H₄ symmetric stretching band in CH₄, determined over a range of pressures from 15 to 5000 psi. Our experimentally determined value for the zero-pressure intercept is 2917.2 cm^{-1} at 25°C (Table A3.1), in excellent agreement with published values of 2917.52 cm^{-1} at 30°C, 2917.01 cm^{-1} at 22°C, and 2917.68 cm^{-1} at 22°C, reported by Lu et al. (2007; Table A3.1).

The density of CH₄ in gas inclusions was estimated using equation A2 from Lu et al. (2007).

$$P(\text{g/cm}^3) = -5.17331E - 05D^3 + 5.53081E - 04D^2 - 3.5187E - 02D \quad (\text{A2})$$

where D is the difference between the measured peak shift and intercept value reported in Table A3.2.

The pressure of CH₄ in gas inclusions was estimated using equation A3 from Lu et al. (2007). This is the pressure at 25°C shown in column 8 of Table A3.2.

$$P(\text{MPa}) = -0.0148 \times D^5 - 0.1791 \times D^4 - 0.8479 \times D^3 - 1.765 \times D^2 - 5.876 \times D \quad (\text{A3})$$

The final reported CH₄ pressures in Table A3.2 were estimated using an equation of state model in PVTsim Nova (revision 4.2, CALSEP A/S, Copenhagen, Denmark), a commercially available software package for simulating the pressure-volume-temperature properties of hydrocarbons, water, and gas mixtures (Christensen, 1999). For CH₄-CO₂

Table A2.1. Fluid Inclusion Homogenization, Eutectic Melting, and Freezing Point Temperatures, for Minerals in Bedding-Parallel Calcite Layers from Wells 1, 2, and 5, Respectively

| Population | T_h hc, °C | API hc, ° | T_h aq, °C | T_m aq, °C | Sal, wt. % | |
|---------------|-----------------|-----------|--------------|----------------|------------|------|
| Well 1 | | | | | | |
| pr; cc | –51 (1) | Gas (L) | | | | |
| | –70 to –75 (20) | Gas (L) | | | | |
| | –35 to –40 (3) | Gas (L) | | | | |
| | –37 to –41 (20) | Gas (L) | | | | |
| | | | 147 (1) | NA | NA | |
| | | | 133 (1) | –19.5 | 22 | |
| sec; cc | | | 80 (1) | NA | NA | |
| | | | 83 (1) | No freeze | NA | |
| sec; sulfate? | | | 142–153 (12) | –19.1 to –22.5 | 21.8–24.0 | |
| | | | 135–140 (5) | –21.1 to –19.1 | 21.8–23.1 | |
| | | | 145–150 (2) | –21.1 to 19.1 | 21.8–23.1 | |
| Well 2 | | | | | | |
| psec; sulfate | –75 to –80 (20) | Gas (L) | | | | |
| | –75 to –80 (20) | Gas (L) | | | | |
| | | | 160–165 (3) | –15.4 to –17.8 | 19.0–20.8 | |
| | | | 152 (1) | –16.3 | 19.7 | |
| | | | NA | –17.4 | 20.5 | |
| | | | 150–155 (2) | –14.8 to –17.0 | 18.5–20.0 | |
| | | | 163 (1) | –17.9 | 20.9 | |
| | | | 160–165 (1) | –19.5 | 22.0 | |
| | | | 155–160 (1) | –16.2 | 19.6 | |
| | | | 140–145 (5) | –16.3 to –17.9 | 19.7–20.8 | |
| | | | 155–160 (5) | –15.7 to –16.4 | 19.2–19.8 | |
| | | | 165–170 (11) | –15.6 (1) | 19.1 (1) | |
| | | | 150–155 (9) | –14.8 to –15.2 | 18.5–18.8 | |
| | | | 165 (1) | –15.1 | 18.7 | |
| | | | 155–160 (7) | 16.0 to –18.5 | 19.5–21.3 | |
| Well 5 | | | | | | |
| psec; sulfate | –46 to –49 (10) | Gas (V) | | | | |
| psec; cc | –74 to –76 (15) | Gas (L) | | | | |
| | –77 to –79 (15) | Gas (L) | | | | |
| psec; sulfate | | | 165 (1) | No freeze | NA | |
| | | | 142–147 (3) | –18.9 to –20.5 | 21.6–22.7 | |
| | | | 158–163 (5) | –19.4 to –20.4 | 22.0–22.7 | |
| | | | 144–149 (5) | –20.1 to –21.2 | 22.4–23.1 | |
| | | | 145–159 (4) | –20.4 to –21.6 | 22.7–23.4 | |
| | | | 138 (1) | –20.8 | 22.9 | |
| | | | 151 (1) | –21.4 | 23.3 | |
| | | | 160 (1) | –21.7 | 23.5 | |
| | | | 170–174 (20) | –20.6 to 22.1 | 22.8–23.7 | |
| | | | 141 (1) | –20.9 | 23 | |
| | sec; sulfate | | | 111 (1) | –22.1 | 23.4 |
| | sec; cc | | | 93–98 (2) | No freeze | NA |
| | | | | 73 (1) | No freeze | NA |
| | | | 74 (1) | No freeze | NA | |
| | | | 88–91 (2) | No freeze | NA | |

Data on the same line indicate coexisting aqueous and petroleum inclusions. The numbers in parentheses are the number of inclusions measured.

Abbreviations: API hc = measured or estimated API gravity of petroleum inclusions; cc = calcite; (L) = homogenization to the liquid phase; NA = could not be determined; pr = primary; psec = pseudo-secondary; Sal, wt. %: salinity computed from NaCl-H₂O system; sec = secondary; T_h aq = homogenization temperature of aqueous inclusions; T_h hc = homogenization temperature of petroleum inclusions; T_m aq = final eutectic melting temperature of aqueous inclusions; (V) = homogenization to the vapor phase.

Table A2.2. Fluid Inclusion Homogenization, Melting, and Freezing Point Temperatures, Respectively, for a Late-Stage Hydrothermal Barite-Cemented \pm Chlorite- and Sphalerite-Bearing Vein in Calcite from Well 2

| Inclusion | Population | T_h aq, °C | T_m aq, °C | T_f aq, °C | Sal, wt. % |
|-----------|-------------|--------------|--------------|--------------|------------|
| OM1 | pr; sulfate | 168 | | | |
| OM2 | pr; sulfate | 176 | | | |
| OM3 | pr; sulfate | 164.6 | | | |
| OM4 | pr; sulfate | 166 | | | |
| OM5 | pr; sulfate | 167 | | | |
| OM6 | pr; sulfate | 165.2 | | | |
| OM7 | pr; sulfate | 166.1 | -44.5 | -18.2 | 21.1 |
| OM8 | pr; sulfate | 163.5 | | | |
| OM9 | pr; sulfate | 163.2 | | | |
| OM10 | pr; sulfate | 169.2 | | | |
| OM11 | pr; sulfate | 166.4 | -47.8 | -18.1 | 21 |
| OM12 | pr; sulfate | 165.9 | | -18.1 | 21 |
| OM13 | pr; sulfate | 162.5 | -45.2 | 16.9 | 20.2 |

The average T_h for this vein was $166.3 \pm 3.6^\circ\text{C}$ ($\pm 1\sigma$; $n = 13$). The data were collected by coauthor Calum I. Macaulay.

Abbreviations: pr = primary inclusion; Sal, wt. % = salinity computed from NaCl-H₂O system; T_f = freezing temperature of aqueous inclusions; T_h aq = homogenization temperature of aqueous inclusions; T_m = final melting temperature of aqueous inclusions.

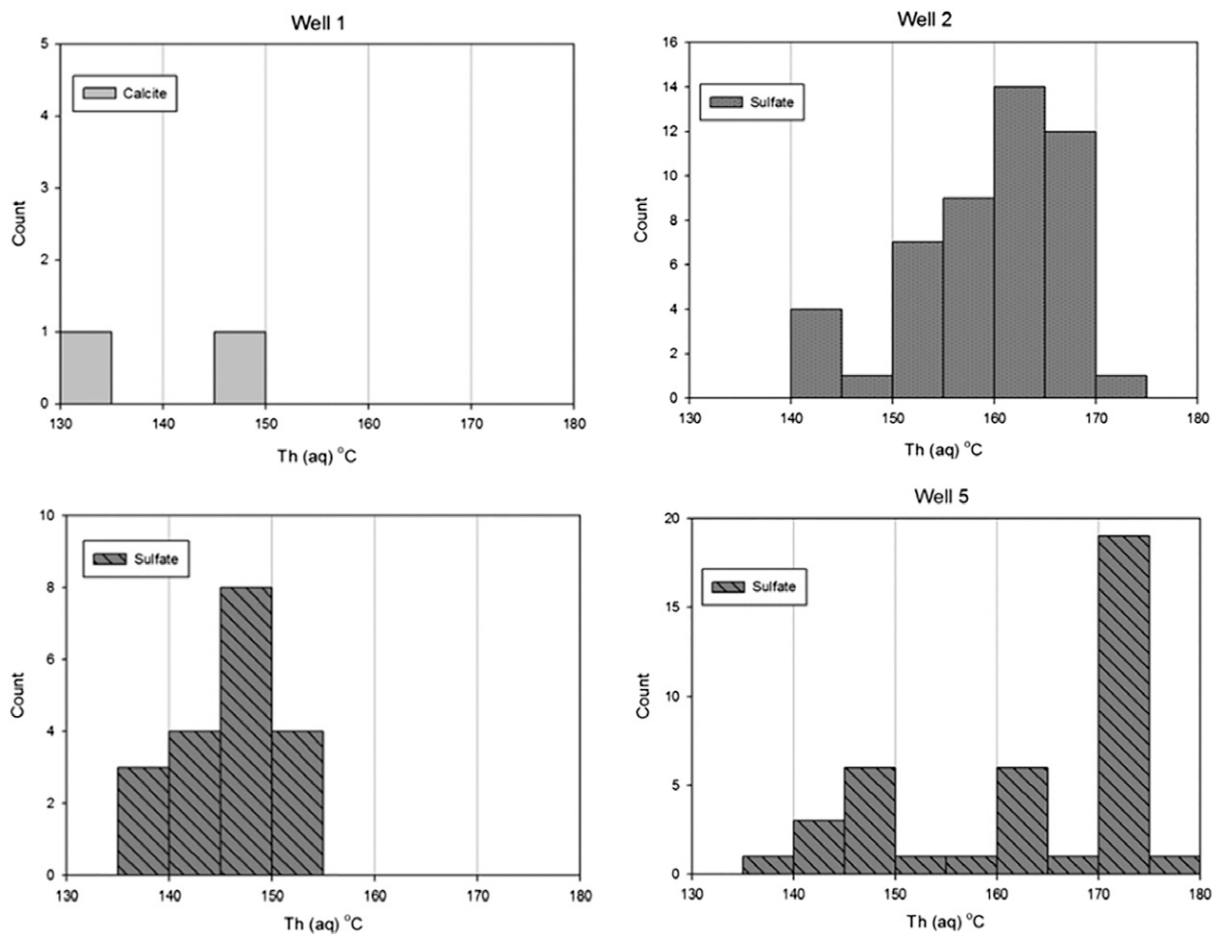


Figure A2.1. Histograms of homogenization temperatures of aqueous fluid inclusions from calcite and sulfate in bedding-parallel calcite layers from wells 1, 2, and 5 in the Haynesville shale. The average homogenization temperature (T_h (aq)) values calculated from these data are as follows: well 1 calcite, 140.0°C; well 1 sulfate, 144.9°C; well 2 sulfate 158.6°C; and well 5 sulfate 162.1°C.

Table A3.1. Calculated CH₄ ν₁ Band Position Near Zero Pressure and Experimental Temperatures

| | References | | | | | | | | |
|--|---------------|---------------|--------------------|---------------|--------------------|-----------------------|----------------|---------------------|-----------|
| | Present Study | CSM, V. Thieu | Thieu et al., 2000 | CSM, M. Jager | Seitz et al., 1996 | Fabre and Couty, 1986 | CSM, K. Hester | Hansen et al., 2001 | Lin, 2005 |
| <i>T</i> , °C | 22 | 21 | 25 | 24 | 25 | 20 | 30 | 22 | 22 |
| <i>v</i> ₀ , cm ⁻¹ | 2918.30* | 2918.65 | 2918.61 | 2918.74 | 2916.61 | 2916.53 | 2917.52 | 2917.01 | 2917.68 |

The references cited herein can be found in Lu et al. (2007).

Abbreviations: CSM = Colorado School of Mines; *T* = temperature; *v*₀ = near zero pressure.

*The second decimal place was inserted to minimize roundoff error during calculations and better reproduce experimental results.

mixtures typical of Haynesville-produced gas (94:6) saturated with water vapor, in situ CH₄ pressures were obtained by iterative simulation until the measured vapor density at 25°C was matched at the FI homogenization temperatures measured on the same FI mineral wafer. A temperature of 160°C was used for well 7 since only CH₄ gas-bearing inclusions were present in samples from this well.

Appendix 4. Oxygen Isotopic Composition of Water

We recognize that the Haynesville shale was deposited in an environment in which gypsum rosettes formed, indicating an arid shallow water to subaerial environment, as described for evaporite formation in the Neuquén Basin by Lo Forte et al. (2005). They analyzed the oxygen and sulfur isotopes in gypsum from the Aconcagu-Neuquén Basin, Argentina (Table A4.1). For gypsum, they report a δ¹⁸O of 13.2‰ ± 1‰ (standard mean ocean water [SMOW]) (*n* = 10; ±1σ). This defines the value of δ¹⁸O_{gypsum}.

With this information and the isotopic fractionation factor α¹⁸O_{gyp-water} from Liu et al. (2019), it is possible to estimate the oxygen isotopic composition of the water involved in gypsum formation. The isotopic fractionation factor for oxygen between gypsum and water (α_{gyp-water}), is given by Liu et al. (2019) as 1.0035 ± 0.0004. They estimated that between 0° and 60°C, the temperature dependence of α¹⁸O_{gyp-water} = -0.000012/°C. This is a negligible

amount, and we therefore adopt the value at 20°C of 1.0035. However, the impact of brine salinity is much larger and needs to be considered. For salinity >150 g/L, Liu et al. (2019) provide the following correction:

$$\delta^{18}\text{O}_{\text{gyp-water}} = \alpha^{18}\text{O}_{\text{gyp-water}} + 1 \times 10^{-5} \times S(S \text{ for salinity} > 150\text{g/L NaCl}) \quad (\text{A4})$$

$$\text{Since } \alpha_{\text{gyp-water}} = \delta^{18}\text{O}_{\text{gyp}} + 1000/\delta^{18}\text{O}_{\text{water}} + 1000 \quad (\text{A5})$$

The oxygen isotopic composition of water may be calculated as

$$\delta^{18}\text{O}_{\text{water}} = [(\delta^{18}\text{O}_{\text{gyp}} + 1000)/\alpha^{18}\text{O}_{\text{gyp-water}}] - 1000 \quad (\text{A6})$$

Using equation A4 and a value of 200 g/L based on measured salinities from aqueous inclusions in BPCLs from Table A2.1, results in an α_{gyp-water} value of 1.0055, which is then used to estimate an average value for δ¹⁸O_{water} of approximately 8‰ (SMOW) given in Table A4.1. This value is consistent with the lower end of the range reported by Weger et al. (2019) of approximately 8.5‰ to 14.5‰ (SMOW).

Adopting a value of δ¹⁸O for water of approximately 8‰ and carbon isotope values of -9‰ to -11‰ (VPDB) from Table A1.1, we estimate from the water-calcite-oxygen isotopic equilibrium of Friedman and O'Neil (1977) a formation temperature range for calcite of

Table A3.2. Estimated Methane Densities and Pressures in Calcite Beef Layers from the Haynesville Shale

| Sample | Depth, ft | CH ₄ :CO ₂ (94:6)-H ₂ O | | | | At 25°C | | At FI <i>T</i> _{hom} | | FPG, psi/ft |
|--------|-----------|--|------------------------------|-----------------------------|-----------------------------|--|-------------------------|-------------------------------|--------|-------------|
| | | Temperature, °C | Peak Shift, cm ⁻¹ | Intercept, cm ⁻¹ | <i>D</i> , cm ⁻¹ | CH ₄ Density, g/cm ³ | P CH ₄ , MPa | P CH ₄ | | |
| Well 1 | 12,614.5 | 145 | 2910.5 | 2917.2 | -6.7 | 0.2758 | 54.1 | 75.98 | 11,020 | 0.87 |
| Well 7 | 12,387.5 | 160* | 2910.8 | 2917.2 | -6.4 | 0.2611 | 46.0 | 72.67 | 10,540 | 0.85 |
| Well 2 | 13,250.1 | 159 | 2910.4 | 2917.2 | -6.8 | 0.2808 | 57.2 | 82.76 | 12,003 | 0.91 |
| Well 5 | 12,318.7 | 162 | 2910.9 | 2917.2 | -6.3 | 0.2563 | 43.7 | 70.89 | 10,280 | 0.83 |

Peak shift refers to the registered CH₄ symmetric stretching mode position for a given sample. The intercept refers to the position of this mode at ambient conditions, and Δ is their difference (*D*), used to estimate fluid density following the procedures in Lu et al. (2007).

Abbreviations: FI = fluid inclusion; FPG = fluid pressure gradient; P = pressure.

Table A4.1. Oxygen and Sulfur Isotopic Compositions of Gypsum from the Aconcagua-Neuquén Basin, Argentina

| Sample | Gypsum | | $\delta^{18}\text{O}$ Water Salinity, g/L | | |
|---|------------------------------|------------------------------|---|-------|-------|
| | $\delta^{18}\text{O}$, SMOW | $\delta^{34}\text{S}$, VCDT | 100 | 200 | 300 |
| A1 | 13.59 | 18.48 | 9.049 | 8.046 | 7.044 |
| A20 | 14.42 | 18.37 | 9.876 | 8.871 | 7.869 |
| A*3 | 13.09 | 17.7 | 8.552 | 7.548 | 6.547 |
| C1 | 13.11 | 18.06 | 8.571 | 7.568 | 6.567 |
| 11C | 13.25 | 17.28 | 8.711 | 7.708 | 6.706 |
| C5 | 11.57 | 18.11 | 7.038 | 6.037 | 5.037 |
| C7 | 11.55 | 17.25 | 7.018 | 6.017 | 5.017 |
| D4 | 14.12 | 17.3 | 9.577 | 8.573 | 7.571 |
| D6 | 13.9 | 17.43 | 9.358 | 8.354 | 7.352 |
| E7 | 13.88 | 18 | 9.338 | 8.334 | 7.332 |
| Average | 13.2 | 17.8 | 8.7 | 7.7 | 6.7 |
| Standard deviation ($n = 10; \pm 1\sigma$) | 1.0 | 0.5 | 1.0 | 1.0 | 1.0 |

Data adapted from Lo Forte et al. (2005).

Abbreviations: SMOW = standard mean ocean water; VCDT = Vienna Canon Diablo Troilite standard.

approximately 140°C to 165°C (Figure A2.1). We note that these temperatures are in excellent agreement with homogenization temperatures measured on aqueous inclusions given in Figure A2.1 and Table A2.1. This temperature range is also broadly consistent with that reported by

Weger et al. (2019) of 120°C to 150°C in mudrocks and 140°C to 195°C for calcite beef layers in the Vaca Muerta Formation. We have observed FI homogenization temperatures as high as 186°C to 200°C in some of our Haynesville samples, but these are not typical.

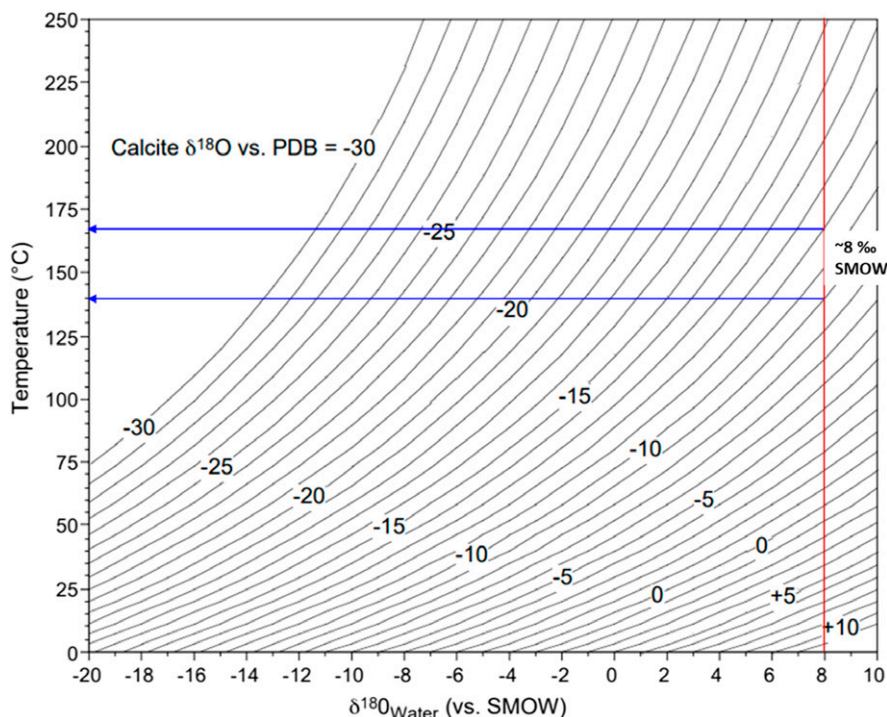


Figure A4.2. Inferred temperatures of the formation of bedding-parallel calcite layers and vertical calcite veins from well 5 in the Haynesville shale. Assuming an oxygen isotopic composition of approximately 8‰ for formation water and using the equilibrium isotopic fractionation model of Friedman and O’Neil (1977) suggests a temperature range of approximately 140°C to 165°C for the formation for the calcite beef layers in the Haynesville shale. PDB = Peedee belemnite; SMOW = standard mean ocean water.

Appendix 5. Molar Volumes of Minerals

Table A5.1. Molar Volume Change for Pseudomorphous Replacement of Gypsum, Anhydrite, and Barite by Calcite

| Replacement Reaction | Molar Volume Change | |
|----------------------|---------------------|-------|
| | cm ³ | % |
| Gypsum→anhydrite | −28.68 | −38.4 |
| Gypsum→calcite | −37.76 | −50.6 |
| Barite→calcite | −15.17 | −29.1 |
| Anhydrite→calcite | −9.08 | −19.7 |

Molar volume data are adapted from Robie and Hemingway (1995).

APPENDICES REFERENCES CITED

- Ault, W. V., and M. L. Jensen, 1963, Summary of sulfur isotope standards, in M. L. Jensen, ed., *Biogeochemistry of sulfur Isotopes*: Washington, DC, National Science Foundation, p. 16–29.
- Christensen, P.L., 1999, Regression to experimental PVT data: *Journal of Canadian Petroleum Technology* v. 38, no. 13, p. 1–9, doi:10.2118/99-13-52.
- Crowe, D. E., and R. G. Vaughn, 1996, Characterization and use of isotopically homogenous standards for in situ laser microprobe analysis of ³⁴S/³²S ratios: *American Mineralogist*, v. 81, no. 1–2, p. 187–193, doi:10.2138/am-1996-1-223.
- Friedman, I., and J. R. O'Neil, 1977, *Compilation of stable isotope fractionation factors of geochemical interest*: Washington, DC, US Geological Survey Professional Paper 440-KK, 117 p., doi:10.3133/pp440KK.
- Liu, T., E. Artacho, F. Gazquez, G. Walters, and D. Hodell, 2019, Prediction of equilibrium isotopic fractionation of the gypsum/bassanite/water system using first-principles calculations: *Geochimica et Cosmochimica Acta*, v. 244, p. 1–11, doi:10.1016/j.gca.2018.08.045.
- Lo Forte, G. L., F. Orti, and L. Rosell, 2005, Isotopic characterization of Jurassic evaporites. Aconcagua-Neuquén Basin, Argentina: *Geologica Acta*, v. 3, no. 2, p. 155–161.
- Lu, W., I.-M. Chou, R. C. Burrus, and Y. Song, 2007, A unified equation for calculating methane vapor pressures in the CH₄-H₂O system with measured Raman shifts: *Geochimica et Cosmochimica Acta*, v. 71, no. 16, p. 3969–3978, doi:10.1016/j.gca.2007.06.004.
- Macnamara, J., and H. G. Thode, 1950, Comparison of the isotopic constitution of terrestrial and meteoritic sulfur: *Physical Review*, v. 78, no. 3, p. 307–308, doi:10.1103/PhysRev.78.307.
- Norlen, G., 1973, Wavelengths and energy levels of Ar I and Ar II based on new interferometric measurements in the region 3400–9800 Å: *Physica Scripta*, v. 8, no. 6, p. 249.
- Ohmoto, H., and R. O. Rye, 1979, *Isotopes of sulfur and carbon*, in H. L. Barnes, ed., *Geochemistry of hydrothermal ore deposits*, 2nd ed.: New York, John Wiley & Sons, 798 p.
- Robie, R. A., and B. S. Hemingway, 1995, *Thermodynamic properties of minerals and related substances at 298.15 K and 1 bar (10⁵ pascals) pressures and at higher temperatures*: Washington, DC, US Geological Survey Bulletin 2131, 461 p., doi:10.3133/b2131.
- Weger, R. J., S. T. Murray, D. F. McNeill, P. K. Swart, G. P. Eberli, R. L. Blanco, M. Tenaglia, and L. E. Rueda, 2019, Paleothermometry and distribution of calcite beef in the Vaca Muerta Formation, Neuquen Basin, Argentina: *AAPG Bulletin*, v. 103, no. 4, p. 931–950, doi:10.1306/10021817384.